Supplementary Material

1 MT Data Analysis

1.1 Data Resolution Depth

The MT method is capable of imaging great depths (up to the upper mantle) significantly more than other active source electromagnetic methods. The depth of penetration of the MT method is dependent on the resistivity of the medium and the period of sounding. The higher the resistivity of the medium, the higher the depth of penetration and the lower the frequency of measurement, the higher the penetration depth. Electromagnetic skin depth is a measure of the depth of the maximum sensitivity of the measured field (Simpson & Bahr, 2005). Long period (low frequency) MT data can be used to image greater depth in the subsurface (up to the mantle). This is because long period electromagnetic waves attenuate slower than short period waves; hence the former penetrates deeper into the Earth.

We carried out depth resolution analysis on the data to investigate the depth to which the MT response is sensitive and can be reliably interpreted. The depths of penetration were calculated using the Niblett-Bostick transformation (Niblett & Sayn-wittgenstein, 1960) to account for variation in depth of penetration for MT sites at similar frequencies. The results of the depth of penetration estimates of the MT data coverage in Botswana for representative periods of 100, 250, 500, and 1,000 seconds are shown in Figure S1. The red colour indicate high depth of penetration of the MT data (between 200 km – 250 km), while the blue colour shows shallower depth of penetration (< 120 km). There is a general increase in the depth of penetration of the MT sites as the period increases, which is evident by more MT sites with high depth of penetration at periods of 500 seconds and 1,000 seconds. At the period of 100 seconds, there are some missing MT sites in the result, whose shortest periods are greater than 100 seconds. The disappearance of some MT sites in the result at longer periods of 500 seconds and 1,000 seconds is due to the lack of long-period data at those sites.

The depth of penetration of the MT data is dependent on the period of recording the MT data and the bulk resistivity of the Earth medium. High bulk resistivity in the subsurface allows for a high depth of penetration of the MT data. Spatially, MT sites that have a relatively higher depth of penetration correspond to stations above cratonic provinces, which have high bulk resistivity values as revealed in the electrical conductivity model. For example, at the period of 250 seconds, higher depth up to 250 km depth is sensed by MT stations above the Congo Craton, Zimbabwe Craton, Rehoboth Province, and Kaapvaal Craton in the northwest, east, west, and south of Botswana, respectively. From the results, the MT data cover in Botswana used in this study can image up to 200 km depth in the subsurface, with 68% of the MT sites having periods above 1,000 seconds.

As the depth of penetration of the MT data becomes higher, the horizontal adjustment length, which is the lateral distance that the MT data is sensitive to increases. At the various depth of penetration of the MT data, the horizontal adjustment length is approximately 2 – 3 times the value of the penetration depth (Simpson & Bahr, 2005). It is then possible to image any subsurface structure that is off the MT data site within the horizontal adjustment length range at a given depth. The results of the 3D country-wide model of this study are discussed along profiles on top or in the near proximity of the MT stations to address the shortcoming of the small horizontal adjustment distance at short periods.

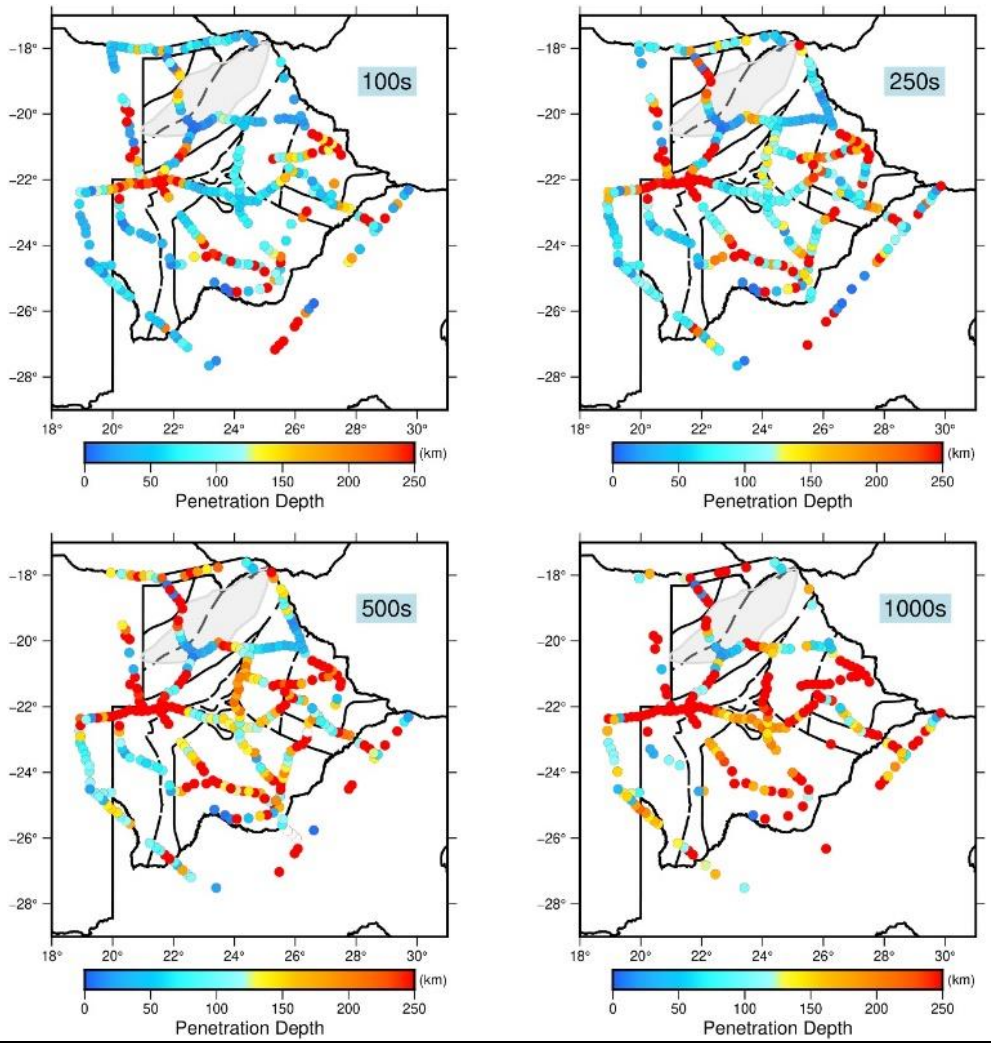

Figure S1: Depth of penetration of the MT data at periods of 100, 250, 500, and 1,000 seconds. The MT sites are represented in circles and the corresponding depths of penetration are indicated by the colour.

1.2 Data Dimensionality

Dimensionality analysis of MT data is an essential step to ensure that the subsurface structure has the same dimensionality as the modelling approach used for the data. In a case where the dimensionality of the MT data is higher than the dimension in which the data is modelled or interpreted (e.g., a 1-D interpretation of a 2-D or 3-D structure), dimensionality distortion occurs in the model, causing inaccurate and erroneous interpretation (Ledo, 2005; Ledo et al., 2002). We carried dimensionality analysis of the data to understand the dimensionality captured in the MT data. The dimensionality analysis was done based on the phase tensor, which is not affected by galvanic distortion as described by Bibby et al. (2005), Booker (2014) and Caldwell et al. (2004). The skew value and ellipticity parameters of the phase tensor were used to analyze the dimensionality. The skew value is a ratio of the amplitudes of the sum of diagonal components to the sum of the off-diagonal components of the impedance tensor. High skew values of the phase tensor greater than 6 º indicate 3-D effects, skew values of 0 º indicate 2-D data, and lower skew values indicate 1-D subsurface structure (Cherevatova et al., 2015; Comeau et al., 2020). The ellipticity of the phase tensor is defined by the ratio of the amplitudes of the sum of diagonal components to the sum of the off-diagonal components of the impedance phase. When the phase tensor is a circle, it indicates 1-D subsurface, while the elliptical phase tensor represents 2-D or 3-D effects in the conductivity distribution (Becken & Burkhardt, 2004; Bibby et al., 2005). A more in-depth description of the parameters of the impedance tensor can be found in Bibby et al. (2005) and Booker (2014).

The results of the phase tensor dimensionality analysis for twelve representative profiles from major geological provinces in Botswana are presented as pseudo section plots in Figure S2, S3, and S4. The pseudo sections are plotted as circles and ellipses, while the colour indicates the skew value of the phase tensor. High skew values greater than 6 º, which are shown in light to dark brown colour, indicate 3-D effects in the data. Also, when the phase tensor's shape is circular, it indicates a 1-D structure, while elliptical phase tensors show 2-D or 3-D effects in the data.

The results of the phase tensor analysis show the presences of 3-D components in the MT data. There is 3-D resistivity structure in most of the MT data sites, which is evident by the high skew values (> 6 º) and elliptical nature of the phase tensor for many of the MT sites, hence the need to model the data in 3-D. The result of this analysis confirms the 3-D nature of the terrane beneath Botswana as reflected in the MT data. The previous MT studies done in Botswana using the SAMTEX data (e.g., Miensopust et al., (2011), Muller et al., (2009), and Khoza et al., (2012)) confirmed the presence of 3-D components in the MT data. There exist multiple principal geoelectric strike directions in the MT data, which is indicative of 3-D structure (e.g., Miensopust et al., (2011), Muller et al., (2009), and Khoza et al., (2012)). For this study, we inverted the MT data in 3-D without need for assumption of geoelectric strike directions, which is required for 2-D modelling.

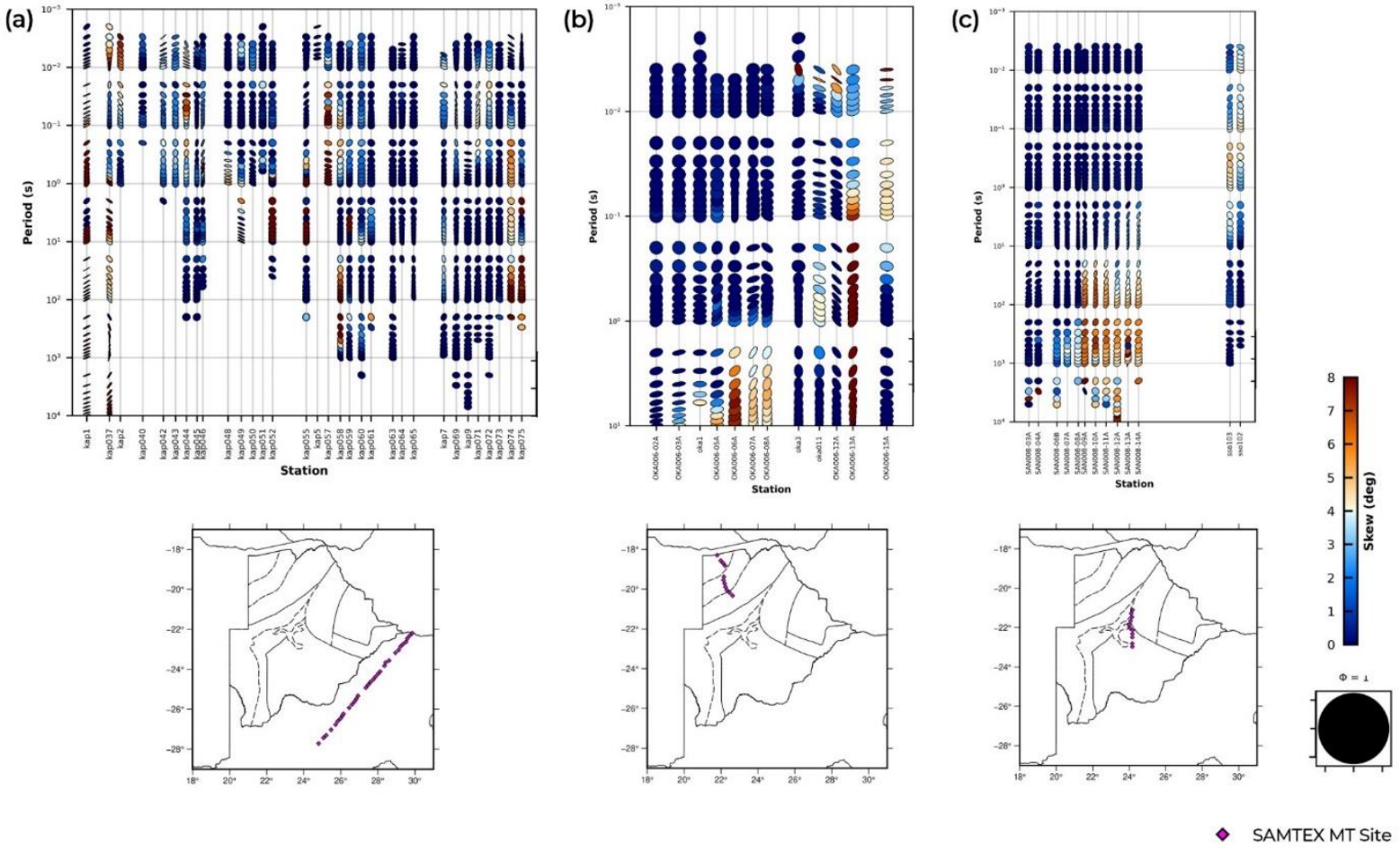

Figure S2: Phase tensor analysis result for three representative profiles. (a-c) Phase tensor ellipses for all periods in MT sites plotted. The corresponding profiles' locations are also shown below each phase tensor ellipse plot with the MT stations' locations as purple diamonds. The phase tensors are plotted left-right or top to bottom along the profiles. The pseudo sections are plotted as circles and ellipses, while the colour indicates the skew value of the phase tensor.

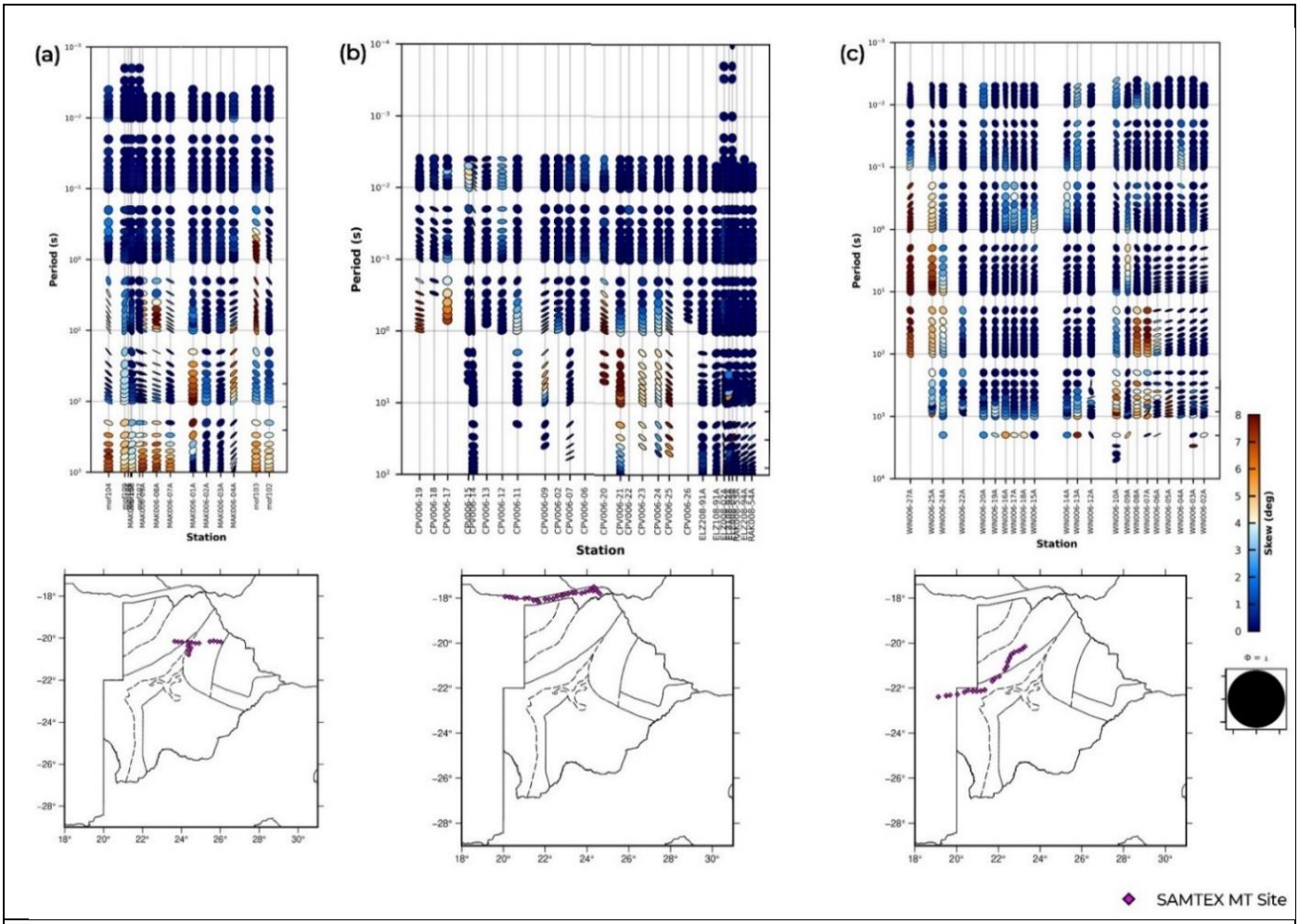

Figure S3: Phase tensor analysis result for three representative profiles. (a-c) Phase tensor ellipses for all periods in MT sites plotted. The corresponding profiles' locations are shown also below each phase tensor ellipse plot with the MT stations' locations as purple diamonds. The phase tensors are plotted left-right or top to bottom along the profiles. The pseudo sections are plotted as circles and ellipses, while the color indicates the skew value of the phase tensor.

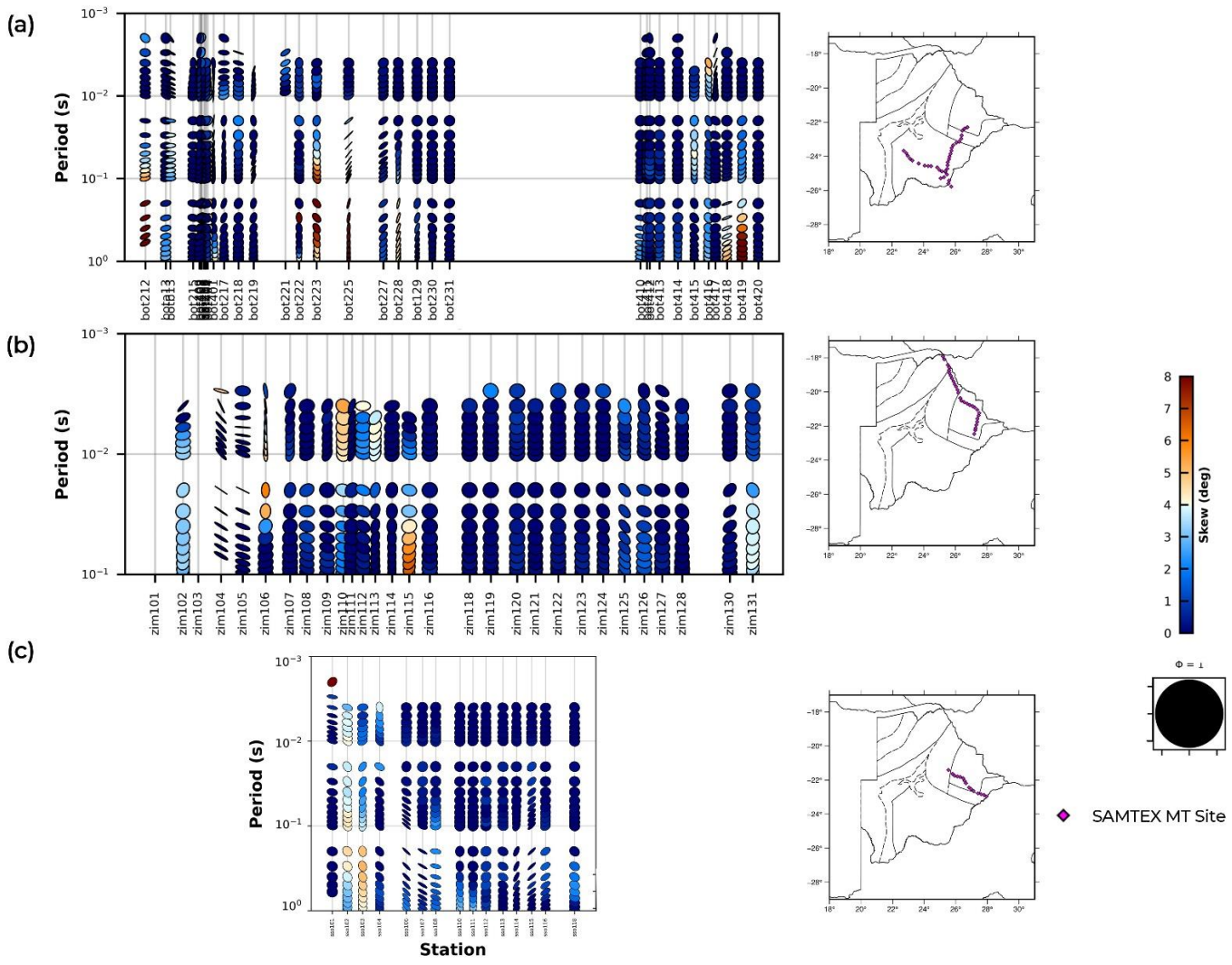

Figure S4: Phase tensor analysis result for three representative profiles. (a-c) Phase tensor ellipses for all periods in MT sites plotted. The corresponding profiles' locations are shown also below each phase tensor ellipse plot with the MT stations' locations as purple diamonds. The phase tensors are plotted left-right or top to bottom along the profiles. The pseudo sections are plotted as circles and ellipses, while the color indicates the skew value of the phase tensor.

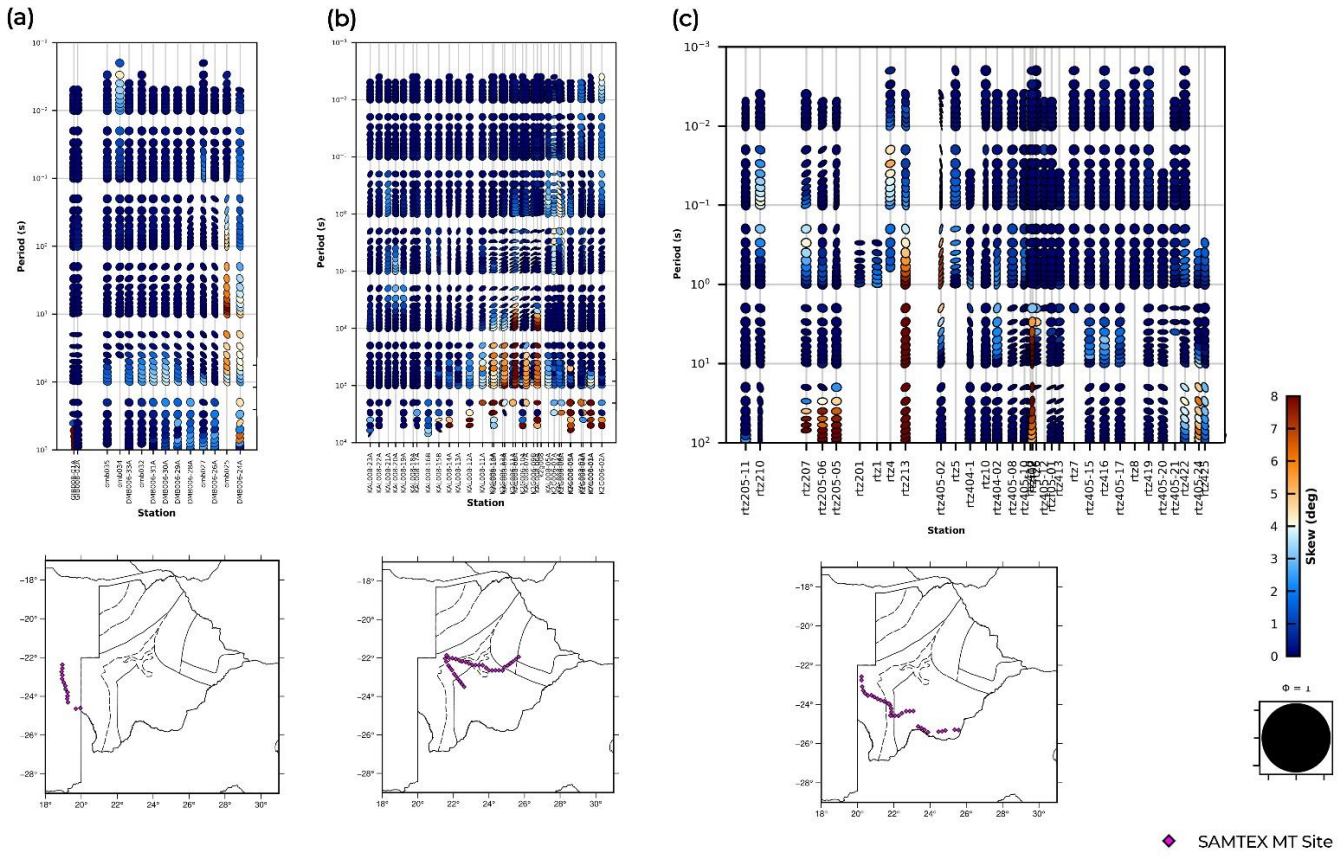

Figure S5: Phase tensor analysis result for three representative profiles. (a-c) Phase tensor ellipses for all periods in MT sites plotted. The corresponding profiles' locations are shown also below each phase tensor ellipse plot with the MT stations' locations as purple diamonds. The phase tensors are plotted left-right or top to bottom along the profiles. The pseudo sections are plotted as circles and ellipses, while the color indicates the skew value of the phase tensor.

2 Sensitivity Tests

2.1 ModEM Inversion Initial Damping Parameter

The ModEM codes allow the user to control the inversion process with the initial damping parameter and inversion computation stopping criterion (Kelbert et al., 2014). The damping parameter controls how the model fits the data progressively in the inversion process (Robertson et al., 2020). As part of this study, a sensitivity test was carried out to investigate how the initial damping parameter affects the resultant model. We used a subset of the MT data consisting of 28 stations in central Botswana for this test to ensure shorter processing time (Figure S6). Initial damping parameters of 1, 10, 100 and 1,000 were tested. We compare the model misfits for the four resultant models (Table S1).

From the results, the nRMS values for the four models are similar. To further gain insight into the resultant models, depth sections corresponding to 7 km, 31 km, and 49 km for the four different models were compared (Figure S6a). Visually, the plan view of depth sections when compared for the four models look similar. However, there is a difference in the number of NLCG iterations required for the model to converge for the different initial damping parameters used. Higher initial damping parameters of 100 and 1,000 took longer NLCG iterations and computation time to achieve convergence of the inversion. The choice of the initial damping parameter has little influence on the resultant model and data misfit. The observations from this sensitivity test are consistent with the results from model space exploration with the Australian Lithospheric Architecture Magnetotelluric Project data using the ModEM codes done by Robertson et al. (2020). For the Botswana country-wide 3-D electrical conductivity modelling, an initial damping parameter of 10 was used to reduce the computing time.

Table S1: Summary of the nRMS for Initial Damping Parameter Sensitivity Test

Initial Damping Parameter	Overall nRMS	Number of NLCG Iteration
1	2.044264	81
10	2.101267	80
100	2.085736	110
1000	2.069875	122

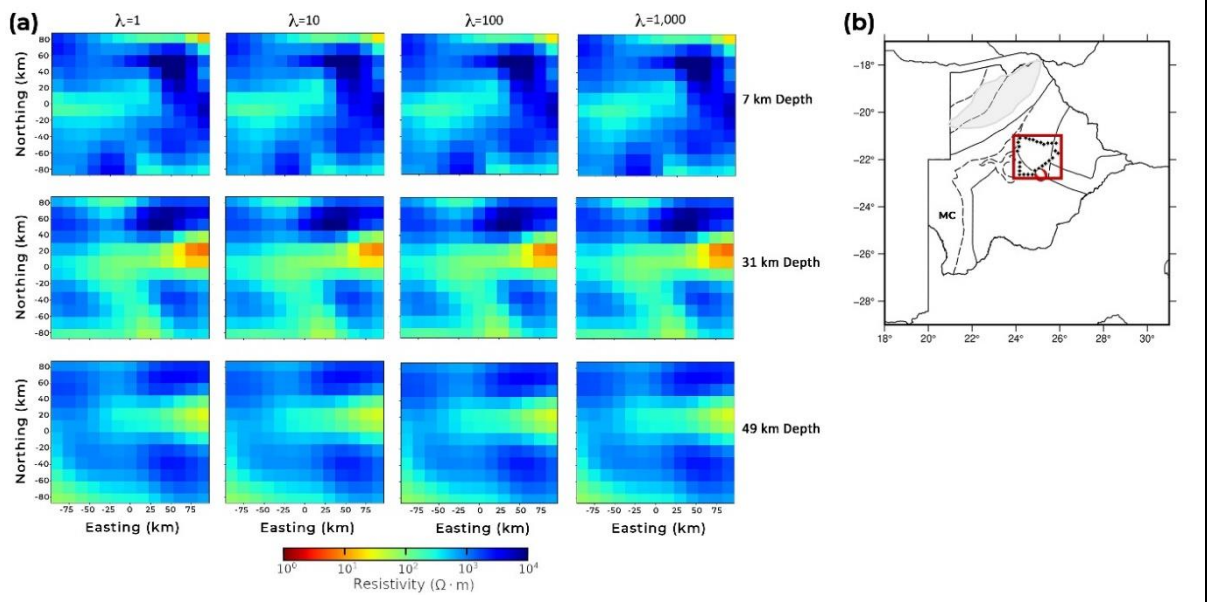

Figure S6: Plan view of electrical conductivity model depth slices at 7 km, 31 km, and 49 km for initial damping parameters of 1, 10, 100, and 1,000 (b) Location Map with the MT stations location as black dots. Red bounding box = location of models presented in (a).

2.2 Model Grid Resolution

Model grid resolution determination is an important step in 3-D MT inversion. The decision of the size of the model grid is usually based on the interstation distances of the stations and a balanced choice between two factors; the need to recover fine model details by using a higher-resolution grid (smaller grid dimension), and the minimization of the computation time and resources required by using coarser grid resolution. In this study, we test the sensitivity of the inversion result to the resolution of the model grid was tested using a dataset covering central and northeast Botswana (Figure S7 and S8). This test was done using a coarse grid of 30 km, an intermediate grid of 15 km and a fine 10 km grid resolutions

We compare the model misfits and the required number of NLCG iterations for the convergence of the three different electrical models with varying resolutions (Table S2). From the results, the overall nRMS decreases with increasing horizontal grid resolution. Increasing the resolution of the grid from 30 km to twice as fine resolution of 15 km has a considerable improvement on the nRMS. Similarly, a further increase in the grid resolution of the model from 15 km to 10 km significantly improved the data fit, which is evident in the reduced nRMS. Figure S9 shows how the MT site nRMS values for all the components of the data (Z and T) compare for the three models per MT sites. The nRMS per site generally decreases with increasing model grid resolution. These results reveal that finer grid model resolution inversion aids better data fit and increase the confidence in the recovered model.

Table S2: Summary of the nRMS for the Model Grid Resolution Sensitivity Test

Model Grid Resolution	Overall nRMS	Number of NLCG Iteration
10 km × 10 km	2.392333	98
15 km × 15 km	3.115478	82
30 km × 30 km	4.067719	74

To further gain insight from how the electrical structures develop in the three different models, depth sections at representative depths in the subsurface were examined. A plan view of the depth sections at 19 km and 49 km from the three models are given in Figure S7 and Figure S8, respectively. From the results of the 19 km depth section, it is revealed that the electrical structures are narrower and less connected in the fine grid model of 10 km. As the model grid resolution becomes coarser (15 km and 30 km), the electrical structures become wider and more connected spatially. Deeper electrical structures are also affected by the reduction of the model grid resolution in similar ways, as shown in the depth sections from 49 km (Figure S8). Also, the finer model shows fine and smooth boundaries of the electrical structures. It is observed that conductive structures are more distinctive at deeper depth in the finer grid model (Figure S8). From these results, it is revealed that finer grid resolution aid the recovery of high-resolution electrical structure with smooth boundaries.

From the results of this sensitivity test, a choice of 10 km grid resolution, which is also the minimum interstation spacing in the data was made for the new nationwide 3-D electrical conductivity modelling in Botswana. This helps to recover a finer model and more realistic model with better data fit. This helps to increase the confidence in the recovered model, which has better data fit and fine spatial resolution.

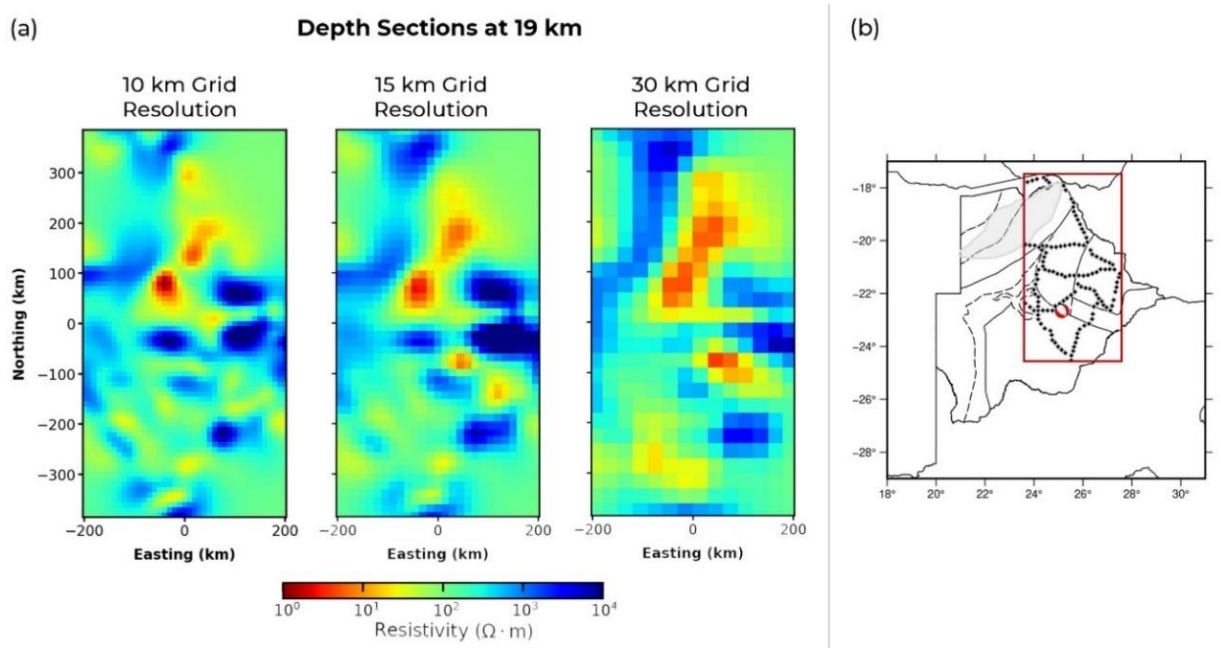

Figure S7: (a) Plan view of electrical conductivity model depth slices at 19 km derived for 10 km, 15 km, and 30 km grid resolution (b) Location Map. Red bounding box = location of models presented in (a).

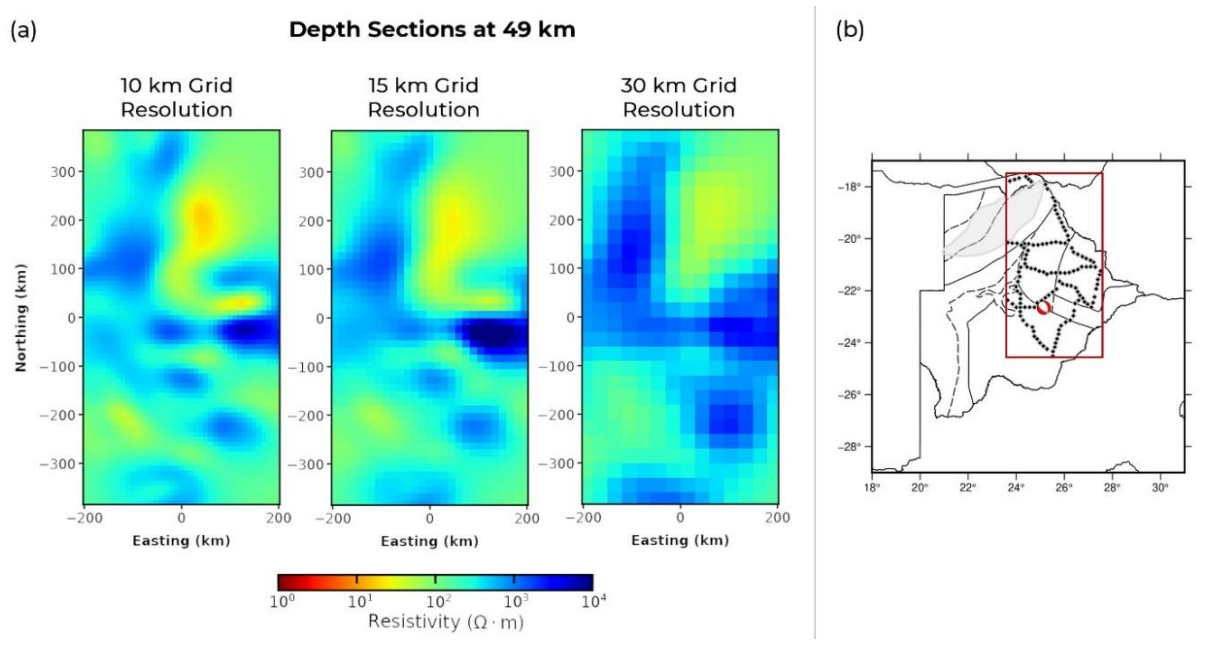

Figure S8: (a) Plan view of electrical conductivity model depth slices at 49 km derived for 10 km, 15 km, and 30 km grid resolution (b) Location Map. Red bounding box = location of models presented in (a).

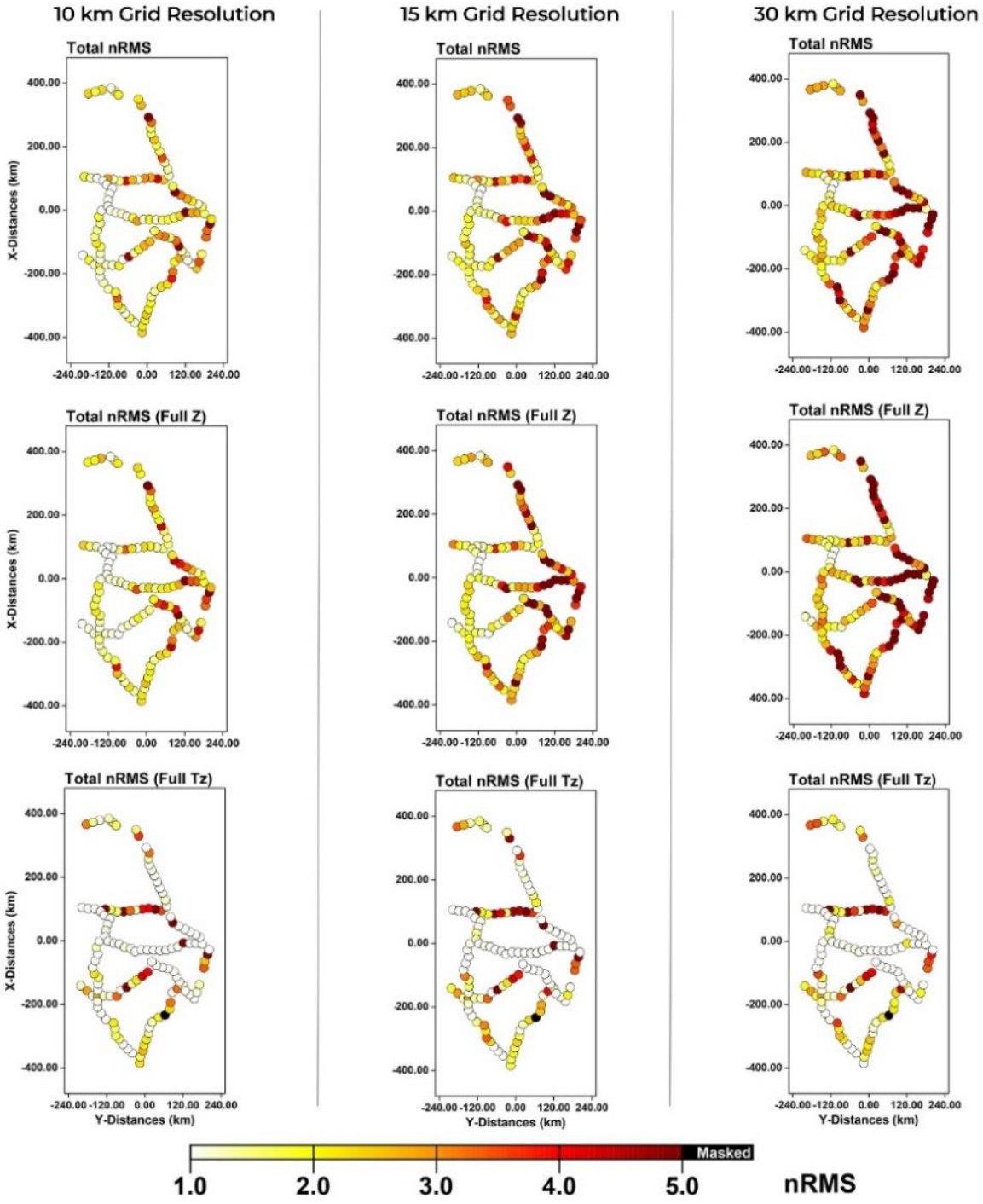

Figure S9: nRMS plot per station for impedance tensor and tipper data components derived for 10 km, 15 km, and 30 km model grid resolutions. The MT sites are represented in circles and the corresponding nRMS are indicated by the colour. Masked sites (shown in black colour) =no data.

2.3 Data Sensitivity of Conductive Structure

The description of this sensitivity test is described in the main text. Here, we repeat the description for the sake of completeness. A major uncertainty in our electrical modelling result was the highly conductive structures (1–10 Ωm) in the lower crust and upper mantle depths. A sensitivity test was carried out to verify the certainty of these high conductivity structures (1–10 Ωm) in the model if they are required in the model and data related. The test involved removing the conductive structures in the model and replacing them with the resistivity of the starting model (100 Ωm). The inversion is then restarted with the modified model. The resultant model was examined to see whether the high conductivity structures are returned in the model or not.

Figure S10 shows the results of the sensitivity test. From the results, it is observed that the high conductivity structures with resistivity values between 1 – 10 Ωm return back to the model after continued inversion of the modified model. This shows that the high conductive structures in the model are required and are data related.

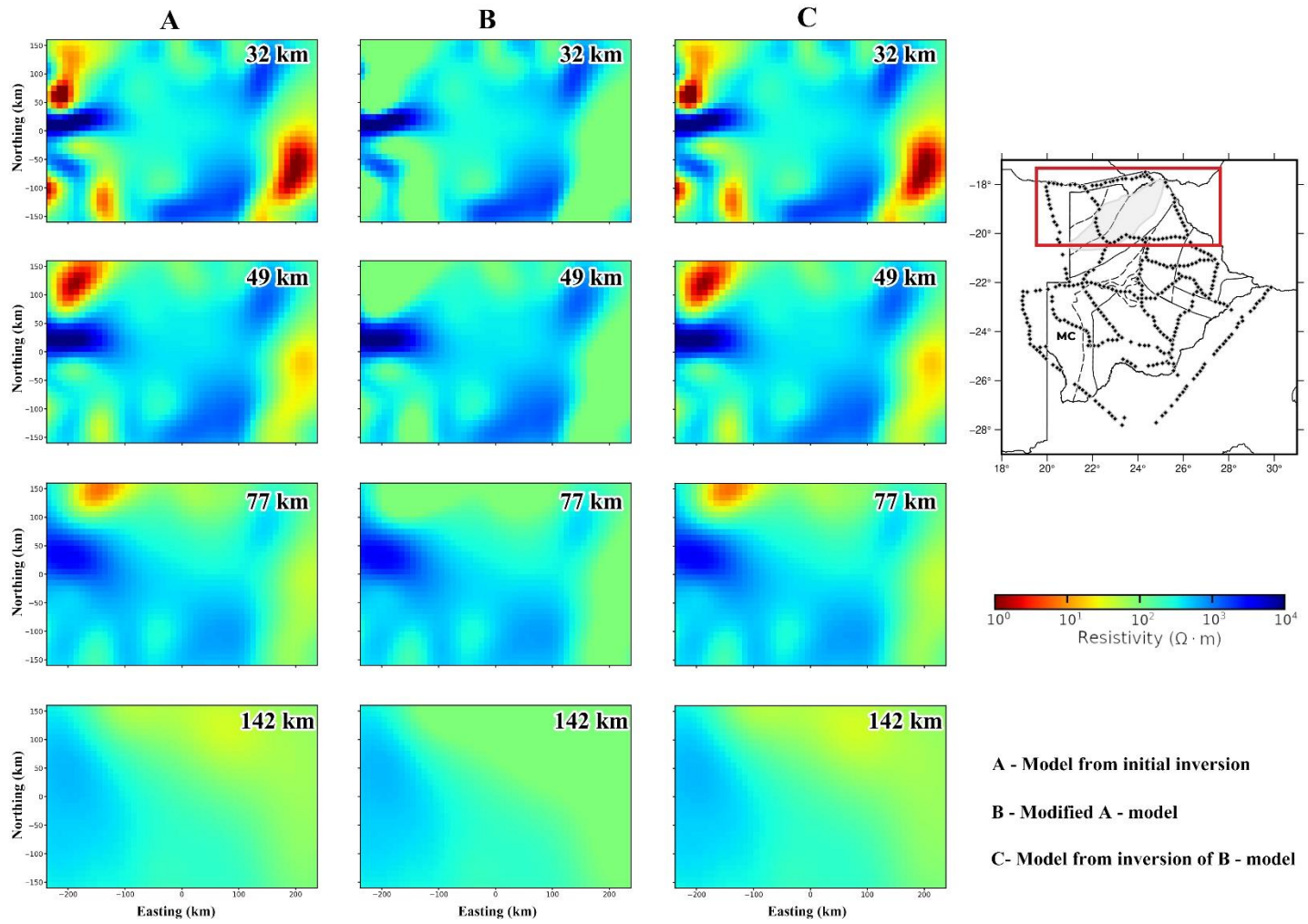

Figure S10: Plan view of electrical conductivity model depth slices at 32 km, 49 km, 77 km, and 142 km derived from model from initial inversion, modified model, and the model from the continued inversion of the modified model.

3 Data fit of the Final Model

3.1.1 Evaluation of Data Fit of the 3-D Nationwide Electrical Conductivity Model

To evaluate the result of the country-wide electrical conductivity model, nRMS analysis of the model was done to examine how it fits the measured MT data. Figure S11 shows the nRMS analysis between the measured MT data and the model-predicted data from the inversion as a function of the MT station for impedance tensor (Z) components, the VTFs components and all the components together. Figure S12 shows nRMS plot per station for each component of the impedance tensor and the tipper. From an examination of the nRMS for the components of the data used, the impedance tensor components have poorer nRMS (3.34) than the VTFs components (2.91). However, there are some sites with poor data fit across the whole dataset for both the impedance tensor and VTFs components, as shown in the total nRMS plots per site. Figure S13 and Figure S14 show the plot of measured and model-predicted responses for representative MT sites that are in close proximity to some of the major tectonic domains. The results show a good fit between the measured and model-predicted data across the whole periods for these representative sites.

From the inversion, the overall nRMS of the nationwide electrical conductivity model is 3.22 after 126 NLCG iterations. The overall nRMS is below the set error floors of 5% used in the inversion process, which is considered good for the model. This error is considered good for a comprehensive dataset in terms of spatial coverage and range of period as this.

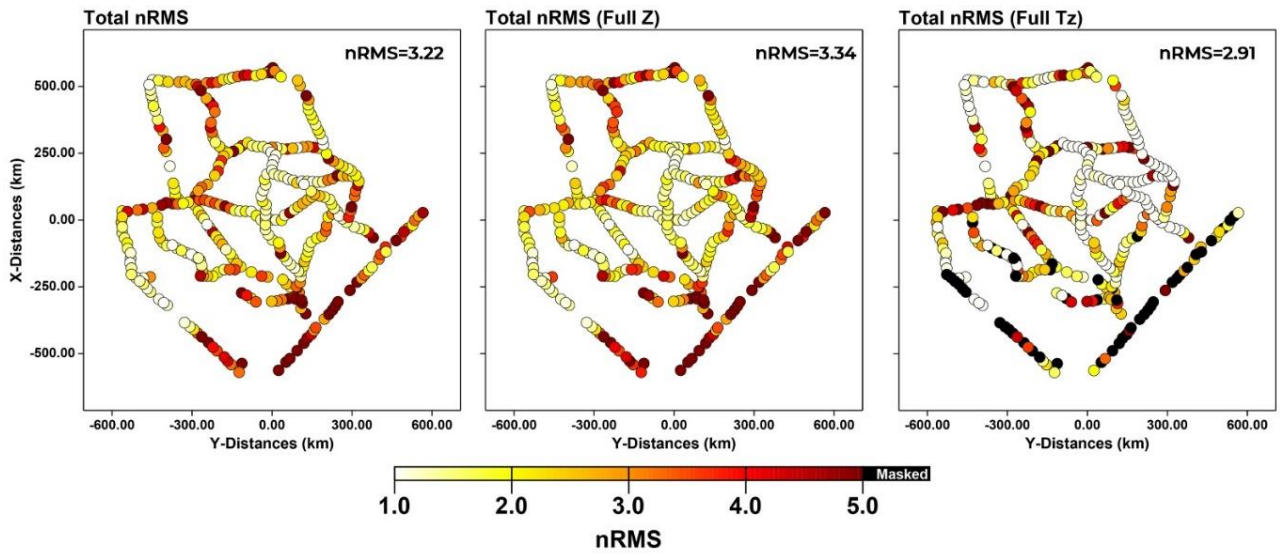

Figure S11: nRMS plot per station for all components of the MT data, impedance (Z) and VTFs. The MT sites are represented in circles, and the corresponding nRMS are indicated by the colour. Masked sites (shown in black colour) = no data.

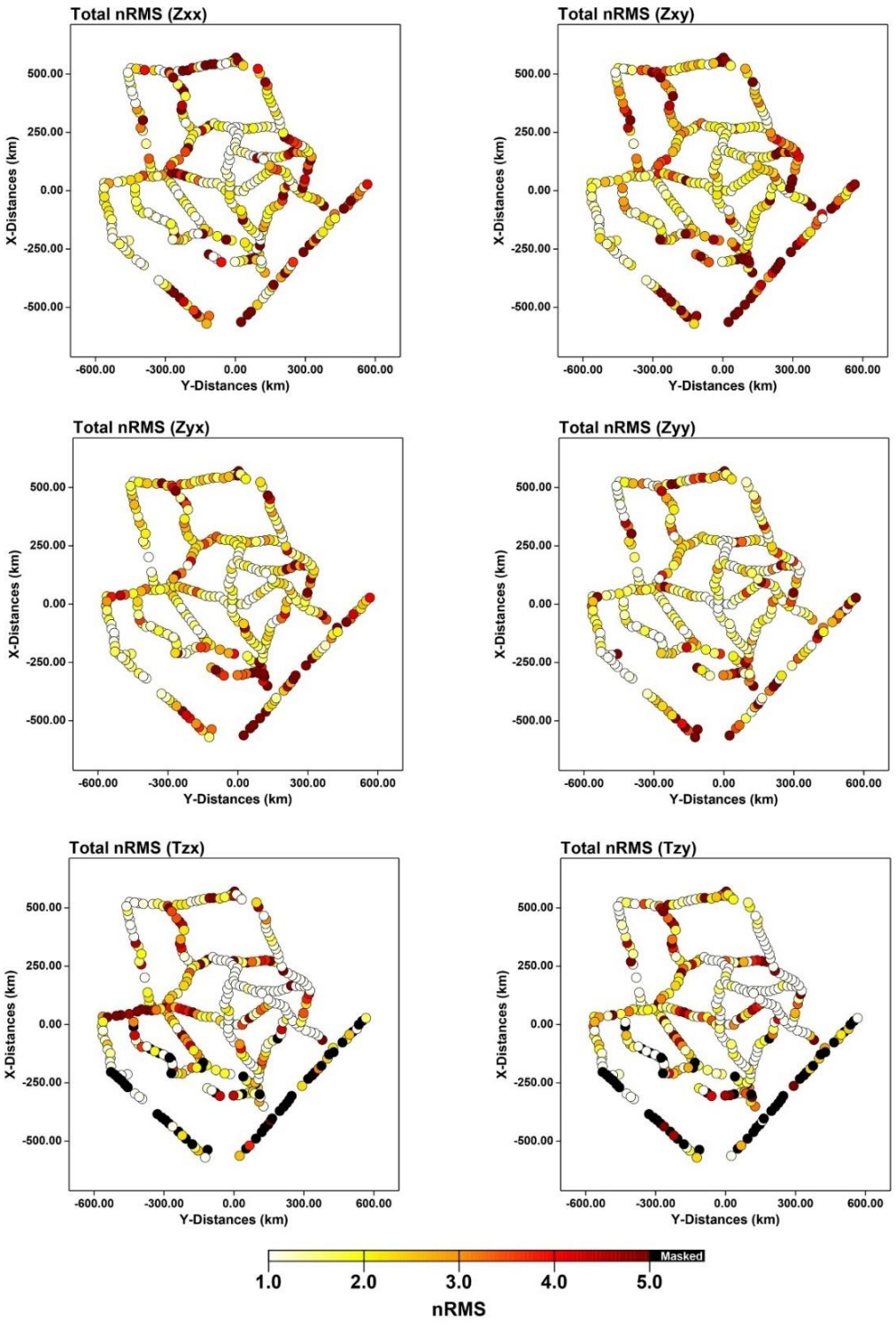

Figure S12: nRMS plot per station for each component of the impedance tensor and VTFs for the 3-D nationwide electrical model of Botswana. The MT sites are represented in circles and the corresponding nRMS are indicated by the colour. Masked (shown in black colour) = no data.

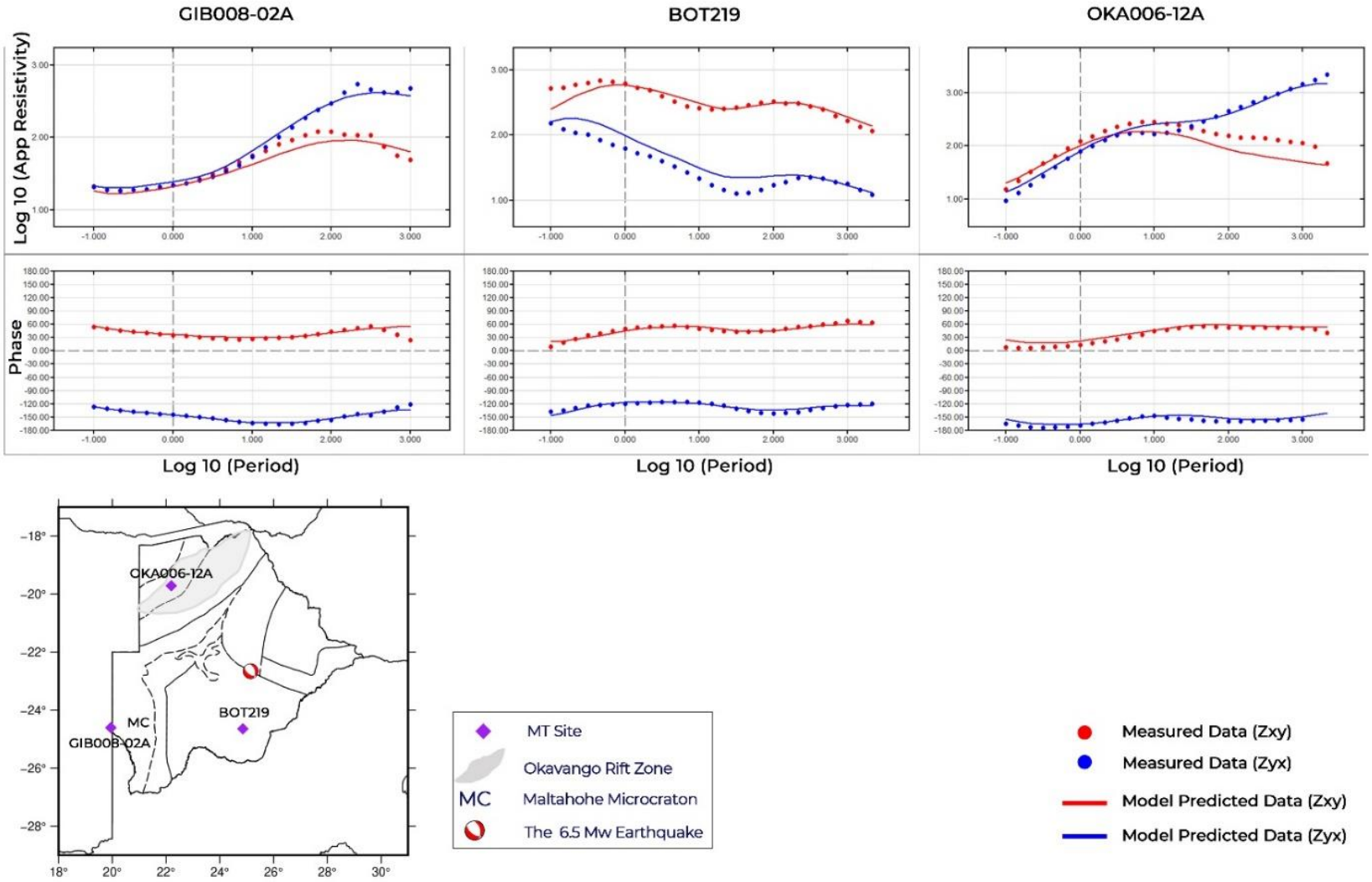

Figure S13: Observed and predicted responses for three representative MT Sites. Location map shows the MT sites analyzed.

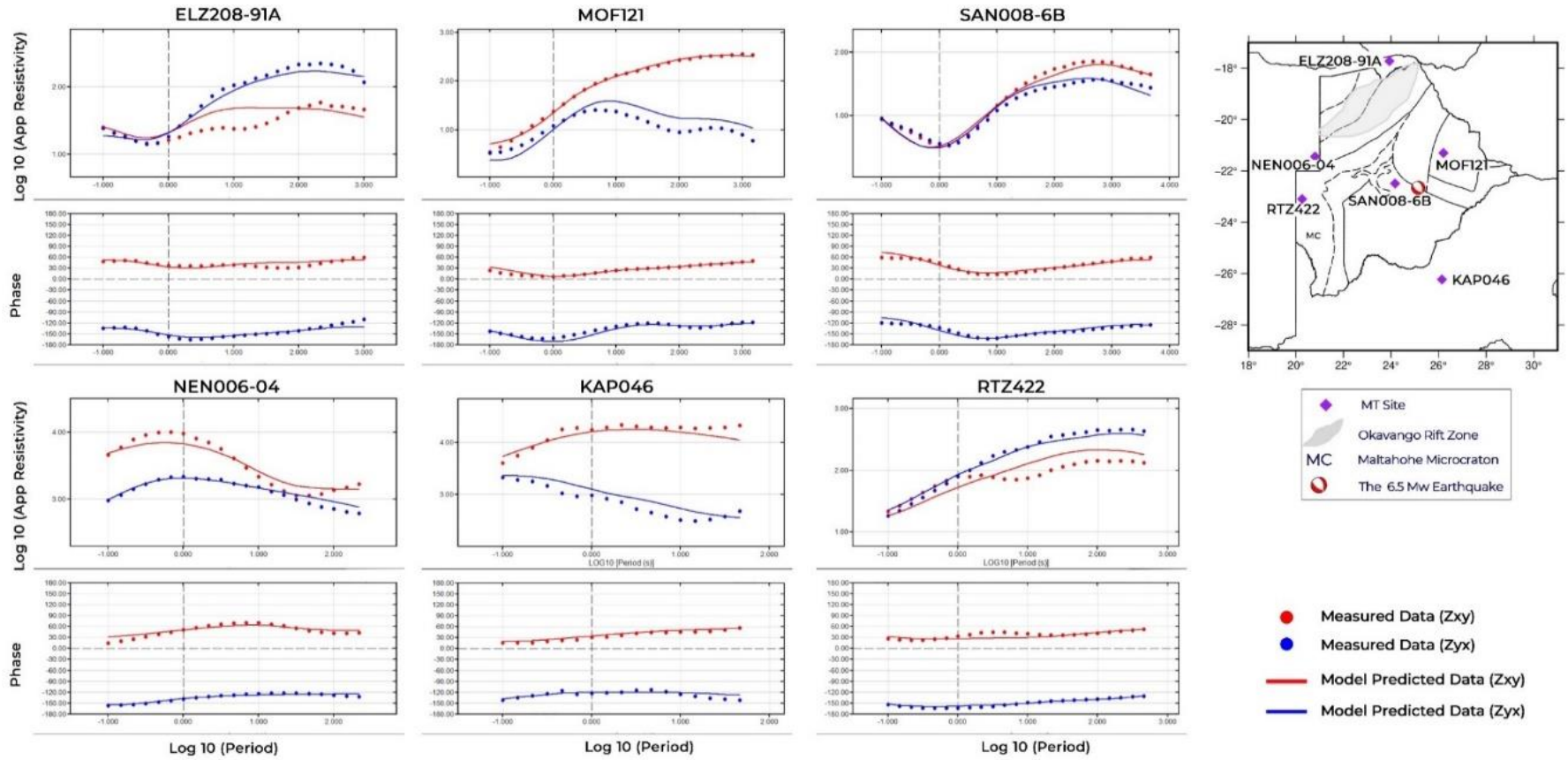

Figure S14: Observed and predicted responses for six representative MT Sites. Location maps shows the MT sites analyzed.